Computing Direct Shadows Cast by Convex Polyhedra

Julien Demouth, Xavier Goaoc

Computing Direct Shadows Cast by Convex Polyhedra

Julien Demouth* Xavier Goaoc†

Abstract

We present an exact method to compute the boundaries between umbra, penumbra and full-light regions cast on a plane by a set of disjoint convex polyhedra, some of which are light sources. This method builds on a recent characterization of topological visual event surfaces presented in a companion paper.

1 Introduction

Since shadows play an important role in human understanding of three-dimensional scenes from two-dimensional pictures [18, 23], their realistic rendering has been a central problem in Computer Graphics for the last decades [12]. While illumination simulation methods such as photon mapping [16] now produce excellent results, it is sometimes desirable to determine shadow boundaries a priori to the illumination simulation, that is, to deduce it from the geometry of the scene. This is the case, for instance, when using shadow volumes [5, 1] for realtime rendering or discontinuity mesh [15, 17] to improve radiosity methods [4, 20]. Unlike hard shadows cast by punctual light sources, whose geometry is well understood [25], soft shadows cast by extended light sources still prove elusive. The classical approach traces shadow boundaries back to *visual event surface* [22], that is points from which the view of the scene changes. The classical visual event surfaces [13], however, capture much more than direct shadows, for example shadows cast by indirect lighting. As a result, methods based on them such as the *discontinuity mesh* [15, 17, 21, 9] or the *visibility skeleton* [11, 10] produce sets of curves that are too large to be used in practice. In this abstract, we present a method that computes exactly the shadows cast by a set of disjoint convex objects, some of which are light sources, ignoring the effects of light reflection which are arguably less important (see, for example, [4]), and evaluate its performances on a few types of random scenes.

*Dept. of Computer Sci. & Eng., POSTECH, Pohang, Korea, julien@postech.ac.kr

†VEGAS Project, INRIA Grand Est, Nancy, France, Xavier.Goaoc@loria.fr

2 Characterization of shadow boundaries

In a companion paper, we studied visual events related to changes in the topology of the apparent contour of a collection of convex sets [8]. Here, we first show that these events are sufficient to capture direct shadows. We then associate to each point of a visual event surface a combinatorial structure, its *germ*, which characterizes the type of change occuring at that point. We show that only points with certain germs can participate in each type of shadow boundary, and that these germs can be associated with the arcs of a graph encoding the visual event surfaces, the visibility skeleton.

Topological visual events. The visual event surfaces are defined as the locus of points at which the view of the scene undergoes a qualitative change. The notions of "view" and "qualitative change" need to be defined carefully, though, as different definitions capture different phenomena. For polyhedral scenes, the view is usually defined as the (abstract) graph obtained by projecting the visible portions of the polyhedra's edges, each element of the graph being labelled by its three-dimensional generators, and two views are qualitatively equivalent if they are isomorphic, as labelled graphs [13]. The corresponding visual event surfaces are of two types [13]: EV surfaces, consisting of origins of rays through a vertex and an edge, and EEE surfaces, formed by origins of rays through three edges (see Figure 1). Thus, the visual event surfaces of a

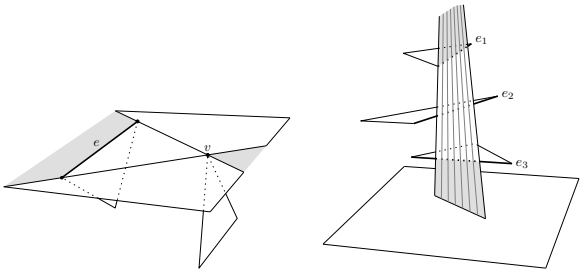

Figure 1: Classical visual event surfaces for polyhedra: EV surface (left) and EEE surface (right).

scene consisting of a single convex polyhedron are the planes supporting its faces. Yet, since the polyhedron is totally visible from anywhere in space, it induces no shadow boundary at all.

These choices of "view" and "qualitative change" are sensitive to the changes in the view not only of the polyhedra, but also of their meshing: events occur whenever a facet starts or ceases to be visible. In a companion paper [8], we studied the visual events corresponding to the topological changes in the apparent contour of a collection of disjoint convex sets. Specifically, we define the view from a point as the set of directions of rays from that point that meet the scene tangentially and declare two such views equivalent if there exists an homeomorphism from the space of direction into itself that maps one view into the other. The associated "topological" visual event surfaces suffice to capture direct shadows.

Theorem 1 *The boundary of the direct shadow cast by a collection of disjoint convex objects is contained in the trace of visual event surfaces corresponding to topological changes in the apparent contour.*

Call a ray *tritangent* if it sees tangentially three objects and *limiting bitangent* if it sees tangentially two objects and lies in a plane tangent to both of them. In the case of disjoint convex polyhedra, we show [8, Theorem 3] that there are two types of such visual event surfaces: EEE surfaces where the three edges come from distinct polyhedra, that is origins of tritangent rays, and EV surfaces where the edge and the vertex come from distinct polyhedra and span a plane tangent to both, that is, origins of limiting bitangent rays.

Germ of a ray. Let ρ be a tritangent or limiting bitangent ray. Up to symmetries, the projection of the the objects seen tangentially by ρ are locally equivalent (that is, homeomorphic) to one of eight basic situations (see Figure 2) which we call the *germ* of ρ; we group the germs into four *types*, from 1 to 4. A ray has one germ for each triple (resp. pair) of

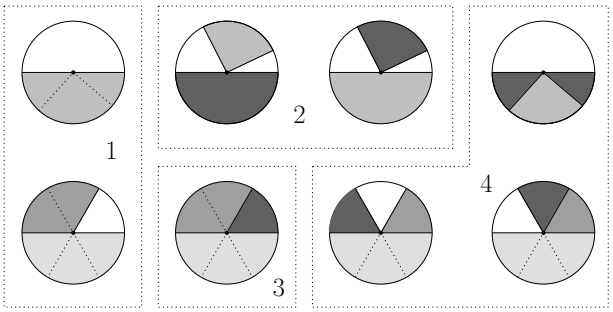

Figure 2: The germs of EV surfaces (top) and EEE surfaces (bottom). Sectors covered by the projection of an object are shaded in grey, lighter colors corresponding to objects closer to the origin of the ray. The numbers $1, \ldots, 4$ indicate the type of the germ(s) of the corresponding box.

object to which it is tritangent (resp. limiting bitangent). Points that belong to a umbra/penumbra or a penumbra/full light boundary are origins of rays with prescribed germ types:

Theorem 2 *A point belongs to the boundary between the umbra and the penumbra (resp. penumbra and full light) regions cast by a collection of convex sets only if it sees a light source tangentially along a ray with germ of type* 1 *(resp.* 2*) or if it sees a light source along a ray with germ of type* 3*.*

Visibility skeleton. Let $\mathcal{C}$ denote a set of convex polyhedra and $A(\mathcal{C})$ the arrangement, in ray space, of the sets of tritangent and limiting bitangent rays. $A(\mathcal{C})$ encodes the visual event surfaces of $\mathcal{C}$ in the sense that these surfaces are the origins of the rays that make up the faces of $A(\mathcal{C})$. Two rays $\rho \subset \rho'$ such that the segment joining their origin does not intersect $\mathcal{C}$ belong to the same cell in $A(\mathcal{C})$. We can thus "collapse" $A(\mathcal{C})$ by identifying all such rays. One way to do that is to consider the quotient space $\mathcal{R}/\sim$ where $\mathcal{R}$ is the space of rays and:

$$(p+\mathbb{R}_+\vec{u}) \sim (q+\mathbb{R}_+\vec{v}) \Leftrightarrow \vec{u} = \vec{v} = \pm\overrightarrow{pq} \text{ and } [pq] \cap \mathcal{C} = \emptyset.$$

The origins of all rays in a given equivalence class make up a *maximal free segment*: a segment that does not intersect $\mathcal{C}$ and is maximal for this property with respect to the inclusion[1]. There is thus a natural bijection between $\mathcal{R}/\sim$ and the space of maximal free segments[2]; we call the image of $A(\mathcal{C})$ under this bijection the *visibility skeleton* of $\mathcal{C}$ relative to topological changes in the apparent contour (by analogy to the classical visibility skeleton [11] defined to encode classical visual event surfaces). For a collection of disjoint convex polyhedra in generic position[3], this visibility skeleton is a graph whose arcs are maximal free segments supported by tritangent or limiting bitangent rays to a given triple/pair of objects, and whose nodes are maximal free segments supported by a line through two vertices (VV node), one vertex and two edges (VEE node) or four edges (EEEE node).

Lemma 3 *Two rays in the same facet of $A(\mathcal{C})$ have the same germ.*

As a consequence, all rays corresponding to a given arc of the visibility skeleton have the same germ, which we call the *germ of the arc*. The characterization of Theorem 2 then extend to arcs of the visibility skeleton, and thus to visual event surfaces.

[1]Note that this differs from the usual definition in that a maximal free segment is not allowed to be tangent to an object.

[2]This bijection is not an homeomorphism as the natural topologies on these spaces differ, but this has no consequence for our purposes.

[3]The same holds for nongeneric position but additional care in the definition is required.

3 Algorithm outline

Our algorithm takes as input a set $\mathcal{C}$ of disjoint convex polyhedra and a plane Π, and consists of 3 steps:

1. Compute the visibility skeleton of $\mathcal{C}$ and the germs of its arcs.
2. Compute the arrangements, in the plane Π, of the curves traced by the surfaces swept by the relevant arcs of the skeleton. We compute two arrangements: (a) with arcs of type 1 tangent to a light source in last position and arcs of type 3 with an endpoint on a light source, and (b) one with arcs of type 2 tangent to a light source.
3. At each curve crossing, remove the arcs not on the shadow boundary locally (see Figure 3).

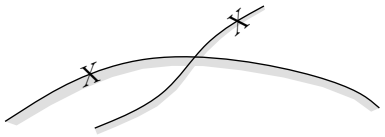

Figure 3: Two arcs incident to a crossing of two curves in arrangement (a) do not belong to the shadow boundary (the shading indicates on which side of the arc the source becomes locally invisible). A similar criterion holds for crossings in arrangement (b).

The output consists of two collections of closed non-crossing loops which, by Theorem 2, contain the boundaries between, respectively, umbra and penumbra – for (a) – and penumbra and full light – for (b). Testing if a given loop is an actual shadow boundary can be done by computing the view of a single point. The visibility skeleton has size $\Theta(n^2k^2)$ [3] and can be computed in time $O(n^2k^2 \log n)$ by a sweep-plane algorithm [14, Chapter 8]. The complexity of the arrangements (a) and (b) is $O(n^3k^3)$ [7], so altogether the algorithm runs in $O(n^3k^3 \log n)$ time in the worst case.

4 Implementation and experimental results

Our implementation was done in `C++` using exact number types and geometrical objects from `CGAL` library. The implementation assumes the objects are in general position in the sense that no 3 vertices are collinear, no 4 vertices (from distinct polyhedra) coplanar and no 10 vertices on a common quadric surface. For Step 1, we compute the VV nodes by brute-force enumeration and use an implementation by Zhang et al. [26] to compute the VEE and EEEE nodes; we retrieve the connectivity using local computations. For Step 2, we use the 2D arrangement package from `CGAL` [24], the arcs of conic curves induced by EEE arcs being described by a rational equation and two algebraic endpoints[4]. See [6, Chapter 6] for a more detailed discussion on the implementation.

We tested three different types of random scenes. In each case, we chose a random collection of k disjoint unit spheres, and for each pick p points on its surface and compute their convex hull. The three types of distribution of centers of spheres that we consider are:

(i) k centers randomly distributed inside a cube,

(ii) k centers randomly distributed on a constant number of horizontal slices of a cube,

(iii) $k-1$ centers randomly distributed on a constant number of horizontal slices of a cone with apex the k^{th} sphere, which is the light source.

We run tests for $k = 10, 30$ and 50 and p ranging between 4 and the greatest power of 2 manageable. Disjointedness is ensured by throwing away centers that violate it and generating them again. For each value of k and p we created 10 scenes for type (i) and a single one for types (ii) and (iii). We analyzed our method using three indicators:

- $gain_1 = \frac{b-a}{b}$, where a denotes the size (number of nodes) of our visibility skeleton and b that of the classical visibility skeleton [11]. It measures the gain obtained by considering "topological" visual events rather than the classical visual events.
- $gain_2 = \frac{d-c}{d}$, where d denotes the number of arcs of our visibility skeleton and c the number of arcs used in Step 2. It measures the effectiveness of the filter based on germ conditions.
- $gain_3 = \frac{e-f}{e}$, where e denotes the complexity of the arrangements (a) and (b) and f that of the output of Step 3. It measures the reduction in size obtained by storing only the (candidate) contours of direct shadows (versus keeping direct discontinuities in the interior of the penumbra).

Our measures show that all three gains are high, most of the time. Specifically,

- $gain_1$ increases with p, reaching 50% for $p = 16$ and 75% for $p = 64$, independantly of k. Since the visibility skeleton has a rather large size, this gain is significant; for instance, for $k = 30$ and $p = 128$, $a = 290000$ and $b = 50000$.
- $gain_2$ is above 85% for all tested scenes, and increases with k.
- $gain_3$ is below 10% for the limit between penumbra and full-light, but above 70% for the limit between umbra and penumbra.

[4]Note that a polygonal approximation of these arcs is performed at visualization.

A comparison of some outputs of our program with images produced using the PBRT rayshooting program [19], represented in Figures 4 and 5 in the Appendix, also suggests that the results are visually convincing. Due to space limitation, we refer to [6, Chapter 6] for a detailed account of the performances.

5 Conclusion

Our experiments suggest that the method we propose is simple enough to be put in practice and leads to significant gains over the classical approach. Of course, these experiments are on small-scale ($\leq 10^4$ triangles) nonrealistic scenes. The main challenges to overcome these limitations include the efficient computation of EEEE nodes and the understanding of "topological" visual events in nonconvex settings. A first progress on the latter was recently made by Batog [2]. Our results also suggest that the boundary of shadow regions is simple enough to be of interest in Computer Graphics.

References

[1] U. Assarsson and T. Akenine-Möller. A Geometry-based Soft Shadow Volume Algorithm using Graphics Hardware. *ACM Transactions on Graphics*, 22(3):511–520, 2003.

[2] G. Batog. *Événements visuels de polyèdres*, Master's thesis, MPRI, ENS Cachan, 2008.

[3] H. Brönnimann, O. Devillers, V. Dujmović, H. Everett, M. Glisse, X. Goaoc, S. Lazard, H.-S. Na and S. Whitesides. Lines and Free Line Segments Tangent to Arbitrary Three-dimensional Convex Polyhedra. *SIAM Journal of Computing*, 37(2):522–551, 2007.

[4] M. F. Cohen and J. R. Wallace. *Radiosity and Realistic Image Synthesis.* Academic Press, 1993.

[5] F. C. Crow. Shadow Algorithms for Computer Graphics. *Computer Graphics*, 11(2):242–248, 1977.

[6] , J. Demouth. *Événements visuels de convexes et limites d'ombres.* PhD thesis, Université Nancy 2, 2008.

[7] J. Demouth, O. Devillers, H. Everett, M. Glisse, S. Lazard and R. Seidel. On the Complexity of Umbra and Penumbra. *Computational Geometry: Theory and Applications*, to appear, 2009.

[8] J. Demouth and X. Goaoc. Topological Changes in the Apparent Contour of Convex Sets. Submitted version available at http://www.loria.fr/∼goaoc/papers/TopVE.pdf. 2009.

[9] G. Drettakis and E. Fiume. A Fast Shadow Algorithm for Area Light Sources Using Backprojection. *Proceedings of ACM* SIGGRAPH *94*, pages 223–230, 1994.

[10] F. Duguet and G. Drettakis. Robust Epsilon Visibility. *Proceedings of ACM SIGGRAPH 2002*, pages 567–575, 2002.

[11] F. Durand, G. Drettakis and C. Puech. The Visibility Skeleton: a Powerful and Efficient Multi-Purpose Global Visibility Tool. *Proceedings of ACM* SIGGRAPH *97*, pages 89–100, 1997.

[12] P. Dutré and K. Bala and P. Bekaert. *Advanced Global Illumination.* A.K. Peters, 2006.

[13] Z. Gigus and J. Malik. Computing the Aspect Graph for Line Drawings of Polyhedral Objects. *IEEE Transactions on Pattern Analysis and Machine Intelligence*, 12(2):113–122, 1990.

[14] X. Goaoc. *Structures de visibilité globales : taille, calcul et dégénérescences.* PhD thesis, Université Nancy 2, 2004.

[15] P. S. Heckbert. Discontinuity Meshing for Radiosity. *Proceedings of the Eurographics Workshop on Rendering*, pages 203–215, 1992.

[16] H. W. Jensen. Global Illumination Using Photon Maps. *Proceedings of the Eurographics Workshop on Rendering*, pages 21–30, 1996.

[17] D. Lischinski, F. Tampieri and D. P. Greenberg. A Discontinuity Meshing Algorithm for Accurate Radiosity. *IEEE Computer Graphics and Applications*, 12(6):25–39, 1992.

[18] P. Mamassian, D. C. Knill and D. Kersten. The Perception of Cast Shadows. *Trends in Cognitive Sciences*, 2(8):288–295, 1998.

[19] M. Pharr and G. Humphreys. Physically Based Rendering: From Theory to Implementation. Morgan Kaufmann, 2004.

[20] F. Sillion and C. Puech. *Radiosity and Global Illumination.* Morgan Kaufmann, 1994.

[21] A. J. Stewart and S. Ghali. Fast Computation of Shadow Boundaries Using Spatial Coherence and Backprojections. *Proceedings of ACM* SIGGRAPH *94*, pages 231–238, 1994.

[22] S. J. Teller. Computing the Antipenumbra of an Area Light Source. *Proceedings of ACM SIGGRAPH 92*, pages 139–148, 1992.

[23] L. R. Wanger. The Effect of Shadow Quality on the Perception of Spatial Relationships in Computer Generated Images. *Computer Graphics*, 25(2):39–42, 1992.

[24] R. Wein, E. Fogel, B. Zukerman and D. Halperin. 2D Arrangements. CGAL User and Reference Manual, Release 3.3, 2007. http://www.cgal.org/Manual/3.3/doc_html/cgal_manual/packages.html#Pkg:Arrangement2.

[25] A. Woo, P. Poulin and A. Fournier. A Survey of Shadow Algorithms. *IEEE Computer Graphics and Applications*, 10(6):13–32, 1990.

[26] L. Zhang, H. Everett, S. Lazard, C. Weibel and S. Whitesides. On the Size of the 3D Visibility Skeleton: Experimental Results. *Proceedings of the Sixteenth Annual European Symposium on Algorithms (ESA 2008)*, to appear, 2008.

A Illustrations

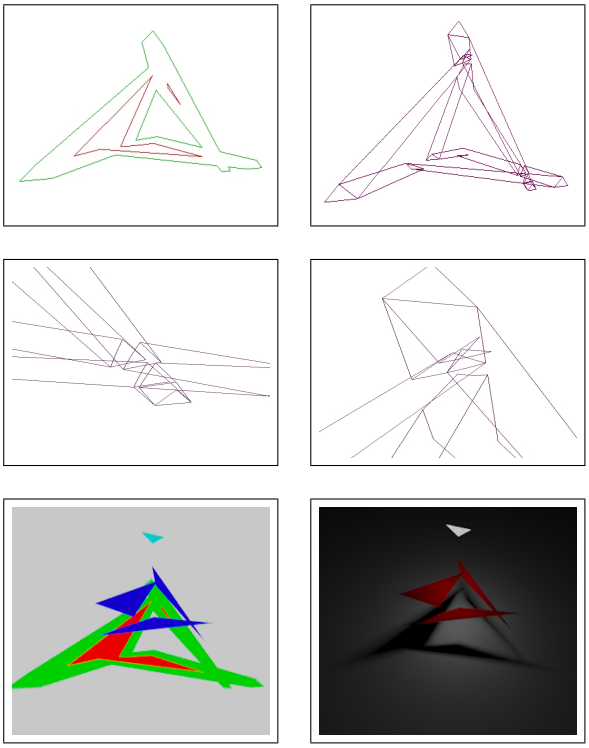

Figure 4: Four triangles, one of which is a light source. Top: output of our algorithm (left) and arrangements obtained after Step 2 (right). Middle: details of the arrangements. Bottom: the three regions obtained by our method (left) and the same scene rendered using a raytracer (right).

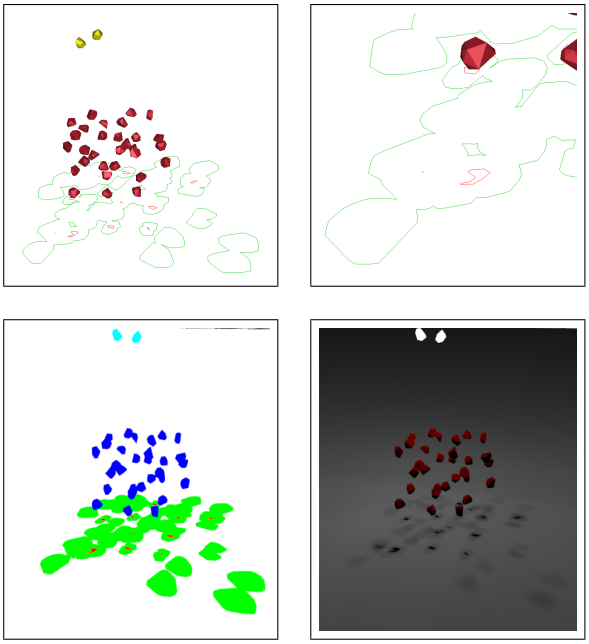

Figure 5: Thirty convex polyhedra, two of which are light sources. Top: output of our algorithm (left) and zoom on a detail (right). Bottom: the three regions obtained by our method (left) and the same scene rendered using a raytracer (right).